Molecular Dynamics Simulation Study of Associations in Aqueous Solutions of Quinuclidine

Arnold Maliniak,[†,‡] Aatto Laaksonen,*[,‡] and Jouko Korppi-Tommola[§]

Contribution from the Division of Physical Chemistry, Arrhenius Laboratory, University of Stockholm, S-106 91 Stockholm, Sweden, and Department of Chemistry, University of Jyväskylä, SF-40100 Jyväskylä, Finland. *Received February 21, 1989*

Abstract: Aqueous solutions of quinuclidine corresponding to 2 and 6 mol %, respectively, are simulated by using a molecular dynamics technique. Both the structural properties and dynamics of the solute and solvent are investigated. The solute molecules form strong hydrogen bonds with the solvent molecules. In the more concentrated solution an aggregation of the solute molecules is observed. The increased structural order of water compared with a pure liquid is found in agreement with other similar systems. The translational motion of water is decreased, whereas the rotational motion is essentially unchanged compared with pure water. The reorientational motion of quinuclidine is clearly anisotropic due to the hydrogen bonds formed with water. The simulated values are also compared with the experimental results obtained from spin relaxation measurements. The translational diffusion coefficients for the solute and solvent molecules are measured with the Fourier-transform pulsed-gradient spin-echo method. In addition, picosecond spectroscopic studies are carried out in order to find experimental evidence of a possible aggregation of quinuclidine molecules in water. These studies show a weak shift in the absorption band in the water solution when the concentration is increased. Also, a dramatic shortening of the fluorescence lifetime is observed. No such behavior, typical of aggregated molecular system, was found in nonpolar solvents.

1. Introduction

None of the nonaqueous solvents possesses all the solvent and ionizing properties water has, especially for ions and polar molecules.[1] Water also has a unique lack of solvent power for many nonpolar substances.[2] Many of these properties are of significance to biological processes. Therefore studies of intermolecular interactions in water and in aqueous solutions are essential to understand the different phenomena occurring in this complex liquid.

Computer simulation studies, in which the interaction can be studied on the molecular level and compared with the experimental results, provide an important source of information. Not surprisingly, a large number of computer simulations of aqueous solutions have been reported in literature. These range from hydration of the smallest anion, electron,[3] and even muonium[4] to extremely complex and highly charged biomolecules such as proteins,[5] DNA,[5,6] and biomembranes[7] as well as simple chemical reactions in water.[8]

The consequences of hydrogen bonds on the structure and dynamics of aqueous solutions have been widely studied by using simulation methods. Both the promotion of water structure, called "structure making", and the disruption or "structure breaking" have been investigated.[9] The detailed information provided on a picosecond time scale on a molecular level is of high significance for studies of hydrogen bonds; it is also difficult to obtain such information from the experiments.

Another problem of crucial importance is the water structure around inert solutes, such as, noble gases, hydrocarbons, and in some other organic substances, readily soluble in many nonpolar solvents. This phenomenon, which is normally called the hydrophobic effect,[2a] is entropically very expensive, because it results in a more ordered water structure around the hydrophobic substance. An overall gain in entropy is obtained if the solute molecules aggregate, thus reducing the hydrophobic surface.

According to MD simulations,[10,11] the translational and orientational motion of the water molecules near nonpolar moieties is slowed down, corresponding roughly to a temperature drop of 20 deg. The hydrogen bond lifetimes in the vicinity of the nonpolar solute are found to increase by a factor of 1.5-2.0.

In this work we report results from molecular dynamics simulation studies of 2 and 6 mol % quinuclidine solutions in water. We also have performed a series of experimental studies by using NMR and picosecond spectroscopy on corresponding (real) solutions for a direct comparison. We have previously used quinuclidine or 1-azabicyclo[2.2.2]octane solutions in both nuclear spin relaxation studies[12,13] and in MD simulations[14,15] as model

† Present address: Weizmann Institute of Science, Rehovot, Israel.
‡ University of Stockholm.
§ University of Jyväskylä.

(1) (a) Bernal, J. D.; Fowler, R. H. *J. Chem. Phys.* **1933**, *1*, 515-548. (b) Frank, H. S.; Evans, M. W. *J. Chem. Phys.* **1945**, *13*, 507-532.

(2) (a) Tanford, C. *The Hydrophobic Effect: Formation of Micelles and Biological Membranes*; Wiley: New York, 1973. (b) Pratt, L. R.; Chandler, D. *J. Chem. Phys.* **1977**, *67*, 3683-3704; **1980**, *73*, 3434-3441. (c) Pangali, C.; Rao, M.; Berne, B. J. *J. Chem. Phys.* **1979**, *71*, 2975-2981; **1979**, *71*, 2982-2990. (d) Ben-Naim, A. *Hydrophobic Interactions*; Plenum: New York, 1980; (e) Goldman, S. *J. Chem. Phys.* **1981**, *74*, 5851-5856. (f) Pratt, L. R. *Ann. Rev. Phys. Chem.* **1985**, *36*, 433-449. (g) Rossky, P. J. *Ann. New York Acad. Sci.* **1986**, *482*, 115-126. (h) Zichi, D. A.; Rossky, P. J. *J. Chem. Phys.* **1986**, *84*, 2814-2822; **1986**, *84*, 2823-2826. (i) Tanaka, H. *J. Chem. Phys.* **1987**, *86*, 1512-1520. (j) Luzar, A.; Bratko, D.; Blum, L. *J. Chem. Phys.* **1987**, *86*, 2955-2959.

(3) (a) Berne, B. J.; Thirumalai, D. *Ann. Rev. Phys. Chem.* **1986**, *37*, 401-424. (b) Schnitker, J.; Rossky, P. J.; Kenney-Wallace, G. A. *J. Chem. Phys.* **1986**, *85*, 2986-2998. (c) Wallqvist, A.; Thirumalai, D.; Berne, B. J. *J. Chem. Phys.* **1987**, *86*, 6404-6418. (d) Schnitker, J.; Rossky, P. J. *J. Chem. Phys.* **1987**, *86*, 3462-3470; **1987**, *86*, 3471-3485. (e) Barnett, R. N.; Landman, U.; Nitzan, A. *J. Chem. Phys.* **1988**, *89*, 2242-2256.

(4) De Raedt, B.; Sprik, M.; Klein, M. L. *J. Chem. Phys.* **1984**, *80*, 5719-5724.

(5) McCammon, J. A.; Harvey, S. C. *Dynamics of Proteins and Nucleic Acids*; Cambridge University Press: Cambridge, England, 1987.

(6) Laaksonen, A.; Nilsson, L. G.; Jönsson, B.; Teleman, O. *Chem. Phys.* **1989**, *129*, 175-185.

(7) Jordan, P. C. *J. Phys. Chem.* **1987**, *91*, 6582-6591.

(8) (a) Chandrasekhar, J.; Smith, S. F.; Jorgensen, W. L. *J. Am. Chem. Soc.* **1984**, *106*, 3049-3050; **1985**, *107*, 154-163. (b) Chandrasekhar, J.; Jorgensen, W. L. *J. Am. Chem. Soc.* **1985**, *107*, 2974-2975. (c) Tapia, O.; Lluch, J. M. *J. Chem. Phys.* **1985**, *83*, 3970-3982. (d) Madura, J. D.; Jorgensen, W. L. *J. Am. Chem. Soc.* **1986**, *108*, 2517-2527. (e) Bergsma, J. P.; Gertner, B. J.; Wilson, K. R.; Hynes, J. T. *J. Chem. Phys.* **1987**, *86*, 1356-1376.

(9) Samoilov, O. Ya. In *Water and Aqueous Solutions*; Horne, R. A., Ed.; Wiley: New York, 1971.

(10) (a) Geiger, A.; Rahman, A.; Stillinger, F. H. *J. Chem. Phys.* **1979**, *70*, 263-276. (b) Alagona, G.; Tani, A. *J. Chem. Phys.* **1980**, *72*, 580-588. (c) Alagona, et al. *Ibid.* **1980**, *72*, 100. Rapaport, D. C.; Scheraga, H. A. *J. Phys. Chem.* **1982**, *86*, 873-880. (d) Rapaport, et al. *Ibid.* **1982**, *86*, 101. Tani, A. *Mol. Phys.* **1983**, *48*, 1229-1240; **1984**, *51*, 161-173. (e) Tani, et al. *Ibid.* 102. Watanabe, K.; Andersen, H. C. *J. Phys. Chem.* **1986**, *90*, 795-802. (f) Watanabe, et al. *Ibid.* **1986**, *90*, 103. (g) Straatsma, T. P.; Berendsen, H. J. C.; Postma, J. P. M. *J. Chem. Phys.* **1986**, *85*, 6720-6727.

(11) (a) Dashevsky, V. G.; Sarkisov, G. N. *Mol. Phys.* **1974**, *27*, 1271-1290. (b) Owicki, J.; Sheraga, H. A. *J. Am. Chem. Soc.* **1977**, *99*, 7413-7418. (c) Swaminathan, S.; Harrison, S. W.; Beveridge, D. L. *J. Am. Chem. Soc.* **1978**, *100*, 5705-5712. (d) Swaminathan, S.; Beveridge, D. L. *J. Am. Chem. Soc.* **1979**, *101*, 5832-5833. (e) Okazaki, S.; Nakanishi, K.; Touhara, H.; Watanabe, N. *J. Chem. Phys.* **1981**, *74*, 5863-5871. (f) Bolis, G.; Clementi, E. *Chem. Phys. Lett.* **1981**, *82*, 147-151. (g) Sheykhet, I.; Simkin, B. *J. Mol. Liq.* **1988**, *37*, 153-165. (h) Jorgensen, W. L.; Buckner, J. K.; Boudon, S.; Tirado-Rives, J. *J. Chem. Phys.* **1988**, *89*, 3742-3746. (i) Rosenberg, R. O.; Mikkilineni, R.; Berne, B. J. *J. Am. Chem. Soc.* **1982**, *104*, 7647-7649. (j) Jorgensen, W. L. *J. Chem. Phys.* **1982**, *77*, 5757-5765. (k) Jorgensen, W. L.; Gao, J.; Ravimohan, C. *J. Phys. Chem.* **1985**, *89*, 3470-3473.

0002-7863/90/1512-86$02.50/0

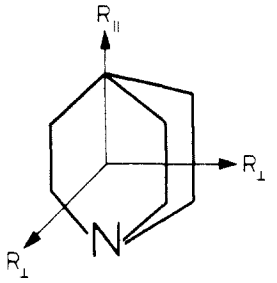

Figure 1. Quinuclidine.

systems for the intermolecular interactions.

Quinuclidine (see Figure 1) is a nearly spherical symmetric rotor molecule with moments of inertia $I_{\parallel} = 3.48 \times 10^{-45}$ and $I_{\perp} = 3.31 \times 10^{-45}$ kgm^2, implying that in the absence of strong intermolecular interactions, the reorientational motion should be nearly isotropic.

The MD simulation of the benzene solution of quinuclidine[15] showed a fairly isotropic reorientation of quinuclidine in accordance with the experiments.[12,13] A highly interesting feature of quinuclidine is the fact that it has both a polar part with an electronegative nitrogen atom and a large (hydrophobic) hydrocarbon surface. Therefore it is a most suitable model molecule to study the various types of intermolecular interactions already discussed above, and their impact on the dynamics of the solute and solvent by varying the polarity of the solvent. Especially in water, quinuclidine is strongly associated with the solvent through hydrogen bonds. The hydrogen bonds will effectively hinder the reorientation perpendicular to the symmetry axis and increase the motional anisotropy. Results from NMR studies of the reorientational motion of quinuclidine in a series of polar and nonpolar solvents are discussed in our earlier papers.[12,13]

In this work we will particularly investigate the hydrophilic and hydrophobic effects responsible to the overall structure and dynamics of both quinuclidine and water molecules. In section 2, we introduce the simulated model system and various technical details from the computations. The experimental techniques and conditions are explained in section 3. In section 4 the simulated results are discussed and compared to the experimental findings. Conclusions are finally drawn in section 5.

2. Physical Model and Computational Details

Constant volume molecular dynamics calculations have been carried out on systems consisting of 20 quinuclidine and 323 and 980 water molecules, corresponding to 2 and 6 mol % solutions, respectively. In addition, we have also performed a simulation of pure water with 343 molecules, to be used as a reference. Both quinuclidine and water are kept rigid during the simulation.

In the present study we use the simple point charge (SPC) model[16] for water–water interactions. This model was originally developed for studies of hydrated proteins and has been later used in a large number of simulations as a solvent model. The SPC model is calibrated under constant volume conditions to reproduce the experimental pressure. The SPC model is reasonably good for structure and thermodynamic properties. For dynamic properties it tends to give too fast a motion according to several simulation studies. For example, the rate of translational diffusion exceeds real values by a factor of two.

The interactions between quinuclidine and water were described by using a Lennard–Jones potential with an electrostatic term

$$U(r_{ij}) = 4\epsilon_{ij}\left\{\left[\frac{\sigma_{ij}}{r_{ij}}\right]^{12} - \left[\frac{\sigma_{ij}}{r_{ij}}\right]^{6}\right\} + \frac{q_i q_j}{4\pi\epsilon_0 r_{ij}} \qquad (1)$$

Table I. Potential Parameters[a]

site	ϵ_{ii} (k_B/K)	σ_{ii} (Å)	q_i ($\|e\|$)
N	46.9	3.32	−0.866
C_α	51.0	3.63	−0.030
C_β	51.0	3.63	−0.440
C_γ	51.0	3.63	−0.220
$H_{\alpha,\beta,\gamma}$	13.4	2.80	0.192
O_W	48.0 (78.199)	3.39 (3.166)	0.820
H_W	0.0	0.0	0.410

[a] Greek subscripts refer to quinuclidine and W to water. The values in the parentheses are the SPC parameters used for water–water interactions.

Table II. Data for the Simulations

	2% solution	6% solution	water
temperature (K)	318 ± 10	309 ± 6	302 ± 7
density (g/cm^3)	0.980	0.980	1.000
box lengths (Å)	32.30	23.89	21.73

where ϵ_{ij} and σ_{ij} are the Lennard–Jones parameters and q_i is the partial charge located on site i. The polar part of the quinuclidine–water potential was constructed by using the interaction energies between ammonia and water from ab initio quantum chemical calculations with a large basis set.[17] Since these calculations did not include a subsequent configuration interaction (CI) calculation, the correlation energy was assumed to be of the same size as that calculated for the water dimer by using the same basis set.[18] The ammonia/water interaction energies were therefore corrected by using water/water dispersion interaction energies. The errors introduced in this procedure should not be too large since it is well-known that the energy of the hydrogen bond is dominated by the electrostatic contribution.[19] This contribution is essentially already included at the SCF level.

The dipole moment of quinuclidine used in the simulation was enhanced compared with the experimental value obtained in a nonpolar solvent (carbon tetrachloride).[20] The dipole moment was scaled by using the bond polarizabilities and the difference in the dielectric constants[21] between water and CCl_4. The dipole moment of quinuclidine in water was taken as 1.31 Debye (D) compared with 1.19 D in CCl_4.[20] The partial charges on quinuclidine were then chosen so as to reproduce the effective value of the dipole moment, while the partial charges on water were the original SPC charges. The same quinuclidine model is also used for the quinuclidine–quinuclidine interactions as in the water–quinuclidine case.

All potential parameters used in this work are gathered in Table I. The cross terms, ϵ_{ij} and σ_{ij}, are derived by using the Lorentz–Berthelot rules.

All simulations were performed in a cubic box, with the periodic boundary conditions and minimum image convention. A cutoff radius of 1 nm is applied to all interactions. The average temperatures and the other data from the simulated system are given in Table II. The equations of motion were integrated with a time step of 0.001 ps, by using the Verlet leap-frog scheme for the translational motion and the quaternion based leap-frog algorithm by Fincham[22] for the rotational motion. All calculations were performed by using a modified version of the computer simulation package "MCMOLDYN".[23]

(12) Maliniak, A.; Kowalewski, J.; Panas, I. *J. Phys. Chem.* **1984**, *88*, 5628–5631.
(13) Maliniak, A.; Kowalewski, J. *J. Phys. Chem.* **1986**, *90*, 6330–6334.
(14) Maliniak, A.; Laaksonen, A. *Mol. Phys.* **1987**, *62*, 489–496.
(15) Maliniak, A.; Laaksonen, A.; Kowalewski, J.; Stilbs, P. *J. Chem. Phys.* **1988**, *89*, 6434–6441.
(16) Berendsen, H. J. C.; Postma, J. P. M.; von Gunsteren, W. F.; Hermans, J. In *Intermolecular Forces*; Pullman, B., Ed.; Reidel: Dordrecht, Holland, 1986.
(17) Diercksen, G. H. F.; Kraemer, W. P.; von Niessen, W. *Theor. Chim. Acta (Berlin)* **1972**, *28*, 67–71.
(18) Diercksen, G. H. F.; Kraemer, W. P.; Roos, B. O. *Theor. Chim. Acta (Berlin)* **1975**, *36*, 249–274.
(19) Umeyama, H.; Morokuma, K. *J. Am. Chem. Soc.* **1977**, *99*, 1316–1332.
(20) Lassier, B.; Brot, C.; Xuong, N. D. *Mol. Phys.* **1974**, *27*, 1697–1700.
(21) Israelachvili, J. N. *Intermolecular and Surface Forces with Application to Colloidal and Biological Systems*; Academic Press: London, 1985.
(22) Fincham, D. CCP5 Quarterly Newsletters. September 1981, No. 2, 6–10.
(23) Laaksonen, A. *Comp. Phys. Comm.* **1986**, *42*, 271–300, Catalog No. AALR.

Table III. The Intermolecular Interaction Energies[a]

	2% solution	6% solution	water
$\langle U_{WW} \rangle$	−39.6 ± 0.6 (−46.1)	−38.5 ± 0.3 (−44.5)	−41.6 ± 1.8 (−46.7)
$\langle U_{QQ} \rangle$	−12.0 ± 0.4 (−0.1)	−31.4 ± 0.3 (3.6)	
$\langle U_{WQ} \rangle$	−98.2 ± 3.4 (−55.9)	−87.8 ± 2.3 (−49.9)	

[a] The values in parentheses are the coulombic contributions (units, kJ/mol).

The systems consisting of 343 and 1000 water molecules were first equilibrated for about 6 ps. Thereafter, 20 water molecules were replaced by quinuclidine molecules, and the density of the new system was adjusted followed by an additional 10 ps of equilibration. The length of the production simulations were 25 ps (12 ps for the pure water simulation). The simulations were performed on FPS-164 array-processor and Convex C210 for the small and large systems, respectively. The electrostatic interactions were treated by using the Ewald summation method.[24]

3. Experimental Section

3.1. Spectroscopic Measurements. Absorption spectra were recorded on a traditional UV-spectrometer (Perkin-Elmer Lambda 5) inerfaced to a personal computer. Fluorescence spectra were recorded by using an excimeter laser-pumped frequency-doubled dye laser output as excitation source and digital BOXCAR detection. Fluorescence lifetime measurements were carried out by using a picosecond spectrometer equipped with single photon counting electronics and a multichannel plate detector.[25] Magic angle detection geometry was used. Deconvolution of the kinetic data was done on a Vax 8600 computer.[26] For fluorescence measurements commercial quinuclidine samples were sublimed twice before recording spectra. Water used in fluorescence measurements was carefully purified and checked for impurities before use.

3.2. NMR Measurements of the Translational Self-Diffusion. The translational diffusion coefficients were obtained from the Fourier-Transform pulsed-gradient spin-echo (FT-PGSE)[27] measurements, performed on JEOL FX100 NMR spectrometer operating at 2.35 T. The experiments were performed on two samples containing 2 and 6 mol % quinuclidine, respectively, dissolved in D_2O; ca. 4 mol % of H_2O was added for enhancement of the signal intensity of water.

3.3. NMR Measurements of the Reorientational Motion. The ^{14}N nuclear spin relaxation measurements were performed at 28.8 MHz on a JEOL GX400 spectrometer; T_2 values were short enough to be determined directly from the line width. The reorientational correlation times of quinuclidine were calculated by using standard equations, assuming the quadrupolar coupling constant to be 4.8 MHz and, according to our previous results,[12,13] independent of the concentration.

3.4. Viscosity Measurements. The viscosities at 25 °C were measured with Cannon–Fenske viscosimeter. The density values necessary for the evaluation of the viscosities were determined at room temperature.

Quinuclidine used in all the experiments was purchased from Aldrich Chemie, Steinheim, FRG. The solvents were of highest spectral purity commercially available and were used without further purification. Twice distilled and degassed water was used to make water solutions.

4. Results and Discussion

4.1. Equilibrium and Structural Properties. The average values of the interaction energies are given in Table III. The water–water energies are per water molecule, and the water–quinuclidine and quinuclidine–quinuclidine energies are per quinuclidine molecule. The electrostatic energies are given in parentheses. In the water–water and water–quinuclidine energies, the dominating contribution comes from the coulombic interactions. This is expected in hydrogen-bonded systems. The quinuclidine–quinuclidine interactions are stabilized by the van der Waals attractions. For the high concentration solution, the coulombic interactions are repulsive. The internal energy for water in quinuclidine solutions is somewhat higher compared to the pure liquid. As expected, the energy for the low concentration solution is intermediate.

The structure of the system is examined by using the radial distribution functions, $g(r_{ij})$. In Figure 2 the relative positions of the atoms O and H in water and N and γ-H in quinuclidine are plotted as g_{ON}, g_{HN}, g_{OH_γ}, and g_{HH_γ}, where the first index refers to water and the second to quinuclidine. The radial distribution functions for the center of mass of water and quinuclidine g_{WQ} are also included in Figure 2. The functions g_{ON} and g_{HN}, which show the radial distribution of water around the nitrogen site, display a sharp first maximum at 0.31 and 0.22 nm, respectively, the second value corresponding to the distance of a hydrogen bond, which is a good agreement compared with X-ray experiments[28] and MC simulations,[29] performed on ammonia–water and other results obtained in similar systems.[30] The second weak maximum in g_{HN} is due to the second proton in the water molecule. The radial distribution function for the two concentrations looks very similar, except for an increase of the intensity in the first maximum of the high concentration solution. The relation between the radial distribution function and the potential of mean force[31] implies that such increase corresponds to a stronger hydrogen bond formed between water and quinuclidine in the 6 mol % solution.

The distribution of water around the γ-hydrogen in quinuclidine is displayed as g_{OH_γ} and g_{HH_γ} in Figure 3b and shows only a weak structure in the radial distribution functions. The small peaks at 0.67 and 0.57 nm, respectively, correspond approximatively to the length of a quinuclidine molecule and can therefore be explained as strong solvation of the polar part of quinuclidine by water. Since no other structure information is observed, this indicates that water has no preferential interactions with the nonpolar part of quinuclidine. There is no concentration dependence in these distribution functions. On the other hand, there is a significant difference between the two concentrations in the center of mass radial distribution functions g_{WQ}. The first maximum in these distributions corresponds to the molecules participating in the hydrogen bond, whereas the second maximum is due to the solvation shell. The intensity of the first maximum is smaller in the dilute solution, in agreement with the other radial distribution functions, g_{ON} and g_{HN}. The large decrease of the intensity with increased concentration can probably be explained by the hydrophobic interactions between the quinuclidine molecules, minimizing contact of the hydrocarbon parts with water.

The total number of water molecules in the first hydration shell around quinuclidine, extended to 0.7 nm, is 14 and 22 for the high and low concentration solutions, respectively. The difference in the hydration numbers probably reflects the attempt of hydrocarbons to minimize contact with water by some kind of aggregation. In Figure 3 the three radial distribution functions for the atoms in water g_{OO}, g_{OH}, and g_{HH} are shown and compared with the distributions in pure water. There is a significant difference in all three distributions with a large increase of water structure in the 6 mol % solution. The distribution functions in the dilute solution are as expected closer to those in pure water. The radial distributions of water over 0.5 nm are essentially identical with these of pure liquid.

A quite similar system, compared to ours, namely a 3 mol % aqueous solution of *tert*-butyl alcohol (TBA) was simulated by Nakanishi et al.[32] Experimentally, TBA was found to have some unique effects on the structure of water,[33] being a very effective "structure maker" and giving arise to a large volume contraction in dilute solutions. In increasing the contraction there is found to be a sharp minimum at 5 mol % in partial molar volume which is assumed to come from an aggregation of TBA in water. As in quinuclidine, TBA has a large hydrophobic surface and a polar –OH group which strongly hydrogen bonds to the water. Na-

(24) (a) Ewald, P. *Ann. Phys.* **1921**, *64*, 253–287. (b) de Leeuw, S. W.; Perram, J. W.; Smith, E. R. *Proc. Roy. Soc. London* **1980**, *A373*, 27–56. (c) Heyes, D. *J. Chem. Phys.* **1981**, *74*, 1924–1929.
(25) Korppi-Tommola, J. To be published.
(26) Program FLUORRES, originally written in Riso, Denmark, was used to deconvolute the fluorescence lifetimes.
(27) Stilbs, P. *Prog. Nucl. Magn. Reson. Spectrosc.* **1987**, *19*, 1–45.
(28) Narten, A. H. *J. Chem. Phys.* **1968**, *49*, 1692–1696.
(29) Tanabe, Y.; Rode, B. M. *J. Chem. Soc. Faraday Trans. 2* **1988**, *84*, 679–692.
(30) *The Hydrogen Bond*; Schuster, P., Zundel, G., Sandorfy, C., Eds.; North-Holland Publishing Company: Amsterdam, Holland, 1976.
(31) McQuarrie, D. A. *Statistical Mechanics*; Harper & Row: New York, **1976**.
(32) *Water, a Comprehensive Treatise*; Franks, F., Ed.; Plenum: New York, 1973.

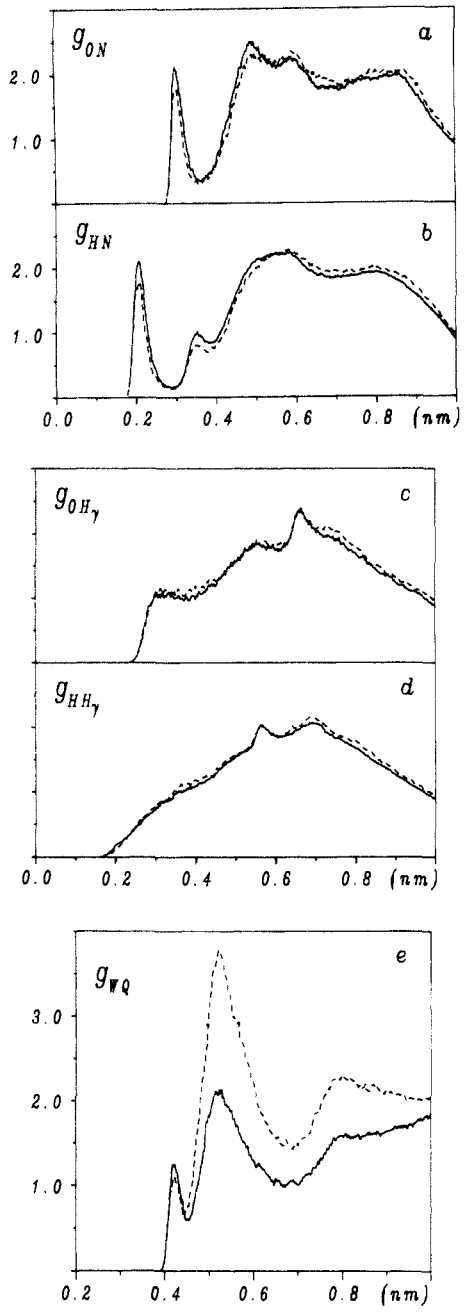

Figure 2. The radial distribution functions, quinuclidine–water: (···) 2 mol % quinuclidine solution and (—) 6 mol % quinuclidine solution.

kanishi et al.[33] report a more pronounced hydrophobic hydration in TBA than in the methanolic water solution which they simulated earlier.[34] Higher intensities in the water–water pair correlation functions in the TBA solution compared to corresponding pair correlation functions in pure water indicate a more structured water, as is found in this work for the more concentrated quinuclidine solution.

Figure 4 shows the radial distribution functions for quinuclidine molecules, g_{NN} and g_{NH_γ}. The functions contain much statistical noise. Nevertheless, some observations can be made. The nitrogen–nitrogen distribution is somewhat sharper in the high concentration solution with a maximum at 0.72 nm. The intensity of nitrogen–γ-hydrogen distribution is essentially larger in the high concentration solution. The dilute solution seems to be homogenous, with the quinuclidine molecules uniformly distributed in the system. The concentrated solution contains most of the

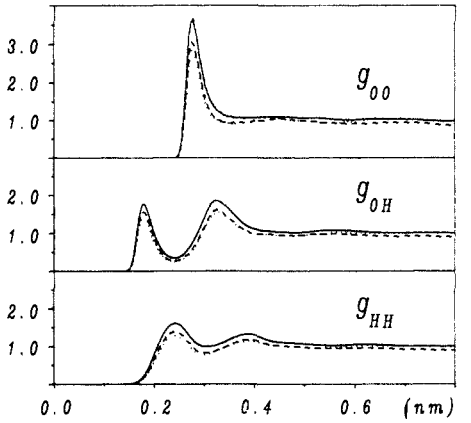

Figure 3. The radial distribution functions, water–water: (– –) 2 mol % quinuclidine solution, (—) 6 mol % quinuclidine solution, and (···) pure water.

quinuclidine molecules in a structure which shows a tendency to aggregate. This association occurs rapidly, a few picoseconds after the simulation is started from a random distribution of quinuclidine molecules. This phenomenon, which is reproducible from different randomly chosen start configurations, does not appear in the simulation of the 2 mol % solution.

For the sake of illustration, but not as evidence, the final configurations from the simulations of the 6 and 2 mol % solutions are plotted in Figure 5 (water molecules are removed for clarity). This association type of phenomenon, which was first observed in the MD simulation and thought to be an artefact, led us to perform more detailed experimental studies at different concentrations. The first observation is that the nonpolar, hydrocarbon parts are associated together, whereas the polar part (nitrogen) points toward water. It seems that the associations minimize the contact of the hydrophobic groups with water, which is also expected in such a high concentration of the hydrocarbon. The aggregation of molecules with a polar and nonpolar, hydrocarbon group is very well-known in the case of amphiphile molecules. Such aggregations have also been investigated by using molecule dynamics simulations.[35,36] However, the geometry of quinuclidine does not favor a regular micelle formation, since there is no effective way of packing the rather bulky hydrocarbon part. On the other hand, the large solubility of quinuclidine in water (>10 mol %) indicates that there must be an efficient way of minimizing the contact between the hydrocarbon part and water. In the initial configuration the quinuclidine molecules are placed randomly in the box. However, considering the high concentration of quinuclidine and its large volume compared with water, the hydrocarbon parts are expected to be very close to each other. Since the contact of hydrocarbon minimizes the free energy of the system, associations observed in this simulation are not surprising. The processes of phase separation, which are controlled by a diffusional step, occur usually on a considerably longer time scale than the length of an MD simulation. In our system the short distances between the quinuclidine molecules in the starting configuration considerably simplify a possible aggregation process.

4.2. Spectroscopic Results. Aggregation of molecules is often accompanied by spectral shifts or by development of entirely new spectral bands as the concentration of the solution is increased.[37] Absorption spectra of quinuclidine in water and in cyclohexane solutions at various concentrations are shown in Figure 6. The absorption maxima around 200 nm are most probably from a $\sigma^*\sigma$ transition. The maximum in water lies below 190 nm, while it is located at 215 nm in cyclohexane. The spectral shift is an

(33) Tanaka, H.; Nakanishi, K.; Touhara, H. *J. Chem. Phys.* **1984**, *81*, 4065–4073.
(34) Okazaki, S.; Touhara, H.; Nakanishi, K. *J. Chem. Phys.* **1984**, *81*, 890–894.
(35) Jönsson, B.; Edholm, O.; Teleman, O. *J. Chem. Phys.* **1986**, *85*, 2259–2271.
(36) Watanabe, K.; Ferrario, M.; Klein, M. L. *J. Phys. Chem.* **1988**, *92*, 819–821.
(37) (a) Lutz, D. R.; Nelson, K. A.; Gochanour, C. R.; Fayer, M. D. *Chem. Phys.* **1981**, *58*, 325–334. (b) Smirl, A. L.; Clark, J. B.; van Stryland, E. W.; Russell, B. R. *J. Chem. Phys.* **1982**, *77*, 631–640. (c) Sundström, V.; Gillbro, T. *J. Chem. Phys.* **1985**, *83*, 2733–2743.

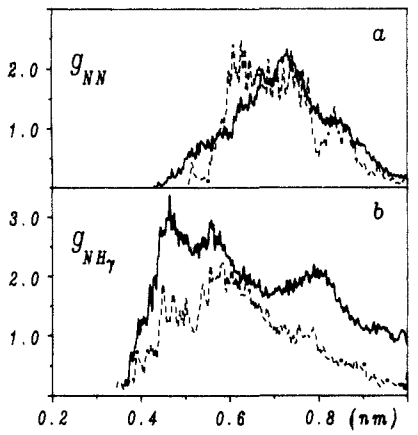

Figure 4. The radial distribution functions, quinuclidine–quinuclidine: (--) 2 mol % quinuclidine solution and (—) 6 mol % quinuclidine solution.

indication of stabilization of the ground state or destabilization of the exciting state of quinuclidine in water solution as compared to cyclohexane solutions. Increasing concentration of water solutions results in an obvious red shift of the spectrum, the major change taking place at about 0.25 mol % concentration. The normalized fluorescence spectra of quinuclidine in water (not shown) also show a red shift as the concentration is increased from 0.5 to 6.0 mol %. No shifts are observed in cyclohexane solutions. The observed shifts are small compared to shifts reported for aggregating dye molecules.[37] These concentration dependent shifts indicate interactions between the quinuclidine molecules at higher concentrations. Kinetic measurements were made by exciting the weak and broad absorption band centered at about 290 nm. This absorption is most probably due to the $\sigma^*\sigma$–n transition and becomes clearly visible at higher concentrations. The lone-pair transition being localized at the polar end of quinuclidine molecule should serve as a sensitive probe of polarity changes of the solvent surroundings. The results of the fluorescence lifetime measurements in water and in benzene are shown in Figure 7. The total decay is fitted to four exponentials. It is clearly seen that increasing concentration in water solution results in a dramatic shortening of the first lifetime component (from 1.3 ns to about 100 ps). The lifetimes of the next two components are also strongly affected. Shortening takes place fairly sharply between concentrations from 0.3 to 0.5 mol %. Similar behavior is observed for the total intensity of the decay signal. These observations are similar to those reported for several aggregating dye molecules in solution.[37] The underlying mechanism of the shortening of the electronic excitation in large molecular aggregates is still under discussion, and in some cases excitation annihilation processes are involved.

4.3. Translational Motion. The translational motion is characterized by using the molecular center of mass velocity time correlation function (tcf), $C_v(t)$, defined by

$$C_v(t) = \langle \bar{v}(0)\bar{v}(t) \rangle / \langle \bar{v}(0)\bar{v}(0) \rangle \qquad (2)$$

where $\bar{v}$ is the linear velocity and $\langle ... \rangle$ is an ensemble average. The translation diffusion coefficient of a molecule may be calculated from the velocity tcf

$$D_v = \frac{1}{3}\int_0^\infty \langle \bar{v}(t)\bar{v}(0) \rangle \, dt = \frac{k_B T}{m}\tau_v \qquad (3)$$

where m is the mass of the molecule or from the mean square-displacement (MSD)

$$\lim_{t\to\infty} \frac{\partial}{\partial t} [\langle [\bar{R}(t) - \bar{R}(0)]^2 \rangle] = 6D \qquad (4)$$

where $R(t)$ is the position of the molecule at time t. In Figure 8 the normalized velocity correlation functions are shown both for components in the mixtures and for pure water. It can be observed in the figure, that there is a difference in the behavior of the correlation functions of water in the mixtures and pure

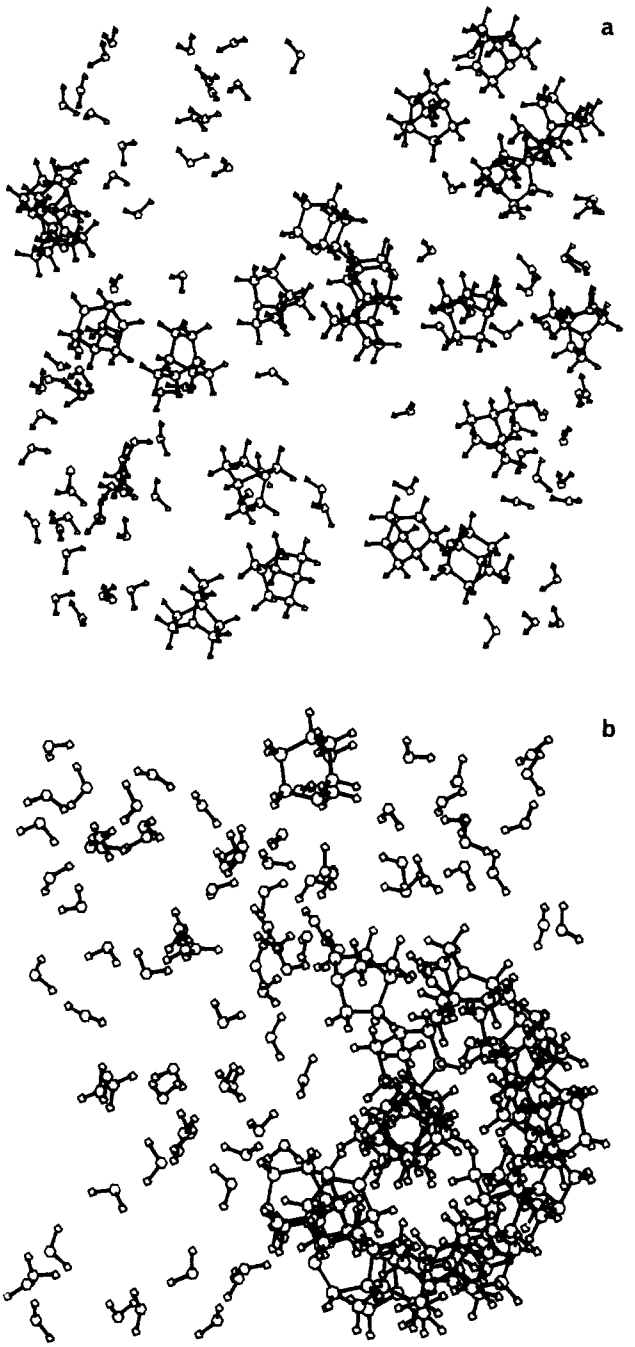

Figure 5. Final configurations from the simulations, (a) 2 mol % solution and (b) 6 mol % solution; 880 and 223 water molecules, respectively, have randomly been removed for clarity.

water. This difference can possibly be attributed to the promoted structuring of water (see also the radial distribution functions) and explained as an increased "cage" effect. These differences are also reflected in the values of the self-diffusion coefficients, which are given in Table IV.

The measurements of the self-diffusion constants were performed on the samples at three different temperatures. The values reported in Table IV are obtained by using the Arrhenius' relation corresponding to 302, 318, and 309 K for pure water, 2 and 6 mol % solution, respectively. As the measurements have been performed in D_2O whereas the simulations are carried out in H_2O, we have included in Table IV the experimental values scaled with the viscosity difference between H_2O and D_2O at the different temperatures.[38] The agreement between the experimental and

(38) Landolt-Börnstein, *Zahlenwerte und Funktionen*; Springer Verlag: Berlin, 1969; Vol. 5a.

Table IV. Self-Diffusion Coefficients[a]

	2% solution			6% solution			pure water		
	$C_v(t)$	MSD	exptl	$C_v(t)$	MSD	exptl	$C_v(t)$	MSD	exptl
quinuclidine	1.5	1.7	0.5 (0.6)	0.6	0.7	0.27 (0.33)			
water	5.0	5.1	2.1 (2.6)	3.7	3.9	1.3 (1.6)	4.3	4.5	1.9 (2.2)

[a] Units, 10^{-9} m^2 s^{-1}. The values in the parentheses are the viscosity scaled diffusion constants.

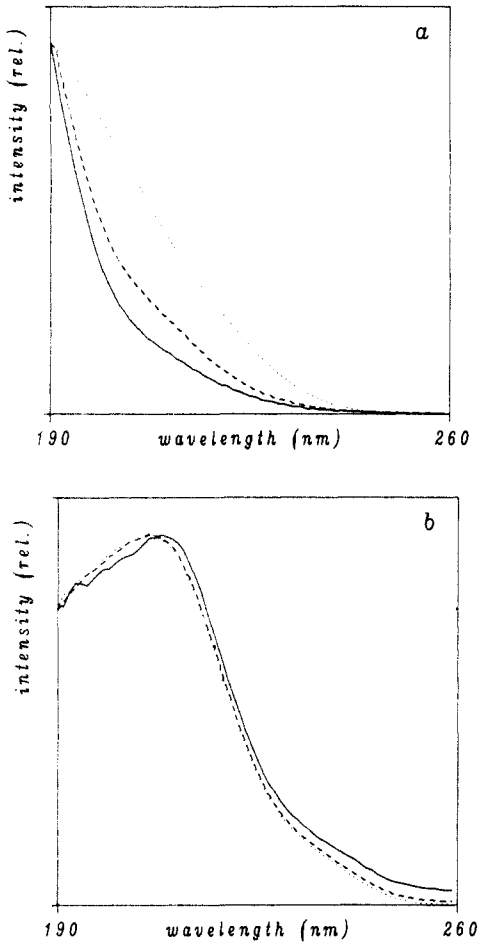

Figure 6. Absorption spectra of quinuclidine in (a) water and (b) cyclohexane ((—) 0.05 mol % quinuclidine solution, (--) 0.15, and (···) 1.50) at various concentrations at room temperature. The spectra have been scaled to correspond to the same absorption intensity at each concentration.

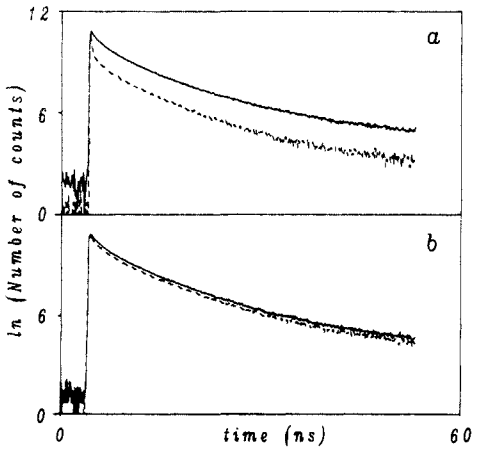

Figure 7. Fluorescence decay curves of quinuclidine in 0.2 and 6 mol% solutions: (a) water and (b) benzene, (--) 0.2 mol % quinuclidine solution and (—) 6.0 mol % quinuclidine solution.

simulated values is rather poor; on the other hand, the ratio is around two and relatively constant for all three systems. It is,

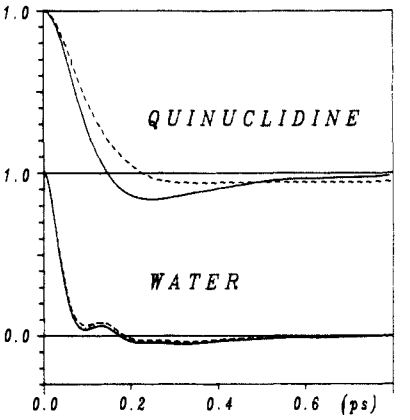

Figure 8. The linear velocity correlation functions: (a) quinuclidine and (b) water, (--) 2 mol % quinuclidine solution, (—) 6 mol % quinuclidine solution and (···) pure water.

of course, well-known that the rigid SPC model for water gives significantly too high a diffusion constant,[16,39] compared with the experimental value. Considering the difference in temperature of the systems, there is a clear decrease in the self-diffusion when the concentration of quinuclidine is increased. The decrease of the self-diffusion coefficient of water in systems where hydrophobic solutes are present has been previously reported, based on computer simulation results[10,40,41] and experimental data.[42]

A significant decrease of the self-diffusion constant of water, measured by tracer and FT NMR techniques,[43] has also been observed in micellar systems. The time correlation functions for the translational motion of quinuclidine are plotted in Figure 8, and the diffusion constants are given in Table IV. There is a large concentration dependence in both simulations and experiments of self-diffusion of quinuclidine in aqueous solutions. There is a significant difference in the behavior of the two correlation functions. In the low concentration solution the correlation function decays more slowly, whereas in high concentration a large cage effect is observed. This effect is explained as the rattling of the molecules back and forth in a cage, due to strong intermolecular forces.[44]

A significant difference in the translational motion of quinuclidine at the two concentrations is also seen from the diffusion constant. Also for quinuclidine the diffusion constants from the simulations are a factor of two too large. The experimental concentration dependence is, however, well reproduced. There is also a difference of a factor of two in the diffusion constants in low and high concentration systems. In 6 mol % water solution we have measured the viscosity at 25 deg and found it to be 3.04 cP compared with 1.4 cP in 2 mol % solution. It seems that the difference in the translational diffusion constants is in good agreement with the viscosity dependence.

4.4. Rotational Motion. The angular velocity time correlation function, $C_\omega(t)$, is defined as

$$C_\omega(t) = \langle \bar{\omega}(t)\bar{\omega}(0)\rangle / \langle \bar{\omega}(0)\bar{\omega}(0)\rangle \qquad (5)$$

where $\bar{\omega}$ is the angular velocity of a molecule. These correlation

(39) Teleman, O.; Jönsson, B.; Engström, S. *Mol. Phys.* **1987**, *60*, 193–203.
(40) Rossky, P. J.; Karplus, M. *J. Am. Chem. Soc.* **1979**, *101*, 1913–1937.
(41) Zichi, D. A.; Rossky, P. J. *J. Phys. Chem.* **1986**, *84*, 2814–2826.
(42) Goldhammer, E. v.; Hertz, H. G. *J. Phys. Chem.* **1970**, *74*, 3734–3755.
(43) Lindman, B.; Kamenka, N.; Puyal, M. C.; Brun, B.; Jönsson, B. *J. Phys. Chem.* **1984**, *88*, 53–57.
(44) Lynden-Bell, R. M.; Hutchinson, D. J. C.; Doyle, M. J. *Mol. Phys.* **1986**, *58*, 307–315.

Table V. Rotational Motion of Quinuclidine

system	T (K)	$\tau_{\omega_\perp}$ (ps)	$\tau_{\omega_\parallel}$ (ps)	τ_{20} (ps)	τ_{21} (ps)	τ_{22} (ps)
2 mol %	318	0.035	0.101	4.3	3.4	2.5
6 mol %	309	0.024	0.044	7.3	5.9	4.0

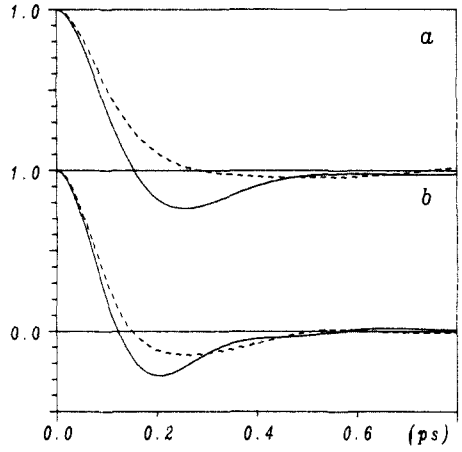

Figure 9. The angular velocity correlation functions for quinuclidine: (a) 2 mol % and (b) 6 mol %, (—) perpendicular component, and (--) parallel component.

functions are related to angular momentum correlation functions and therefore determined by the torques due to other molecules in the liquid. This is the reason why the angular velocity tcfs are a sensitive probe of intermolecular interactions. Figure 9 shows the angular velocity correlation functions for quinuclidine in both high and low concentration simulation. The angular velocity of the center of mass has been resolved into the components of the molecular coordinate system. For symmetric rotors, such as quinuclidine, there are two equivalent axes denoted as perpendicular and one parallel axis. The definitions of parallel and perpendicular components refer to the axis of symmetry of the molecule.

The perpendicular component shows a pronounced cage effect, whereas the parallel component clearly indicates that this rotation is less hindered. The difference can also be seen from the angular velocity correlation times, τ_ω, obtained as integrals of the time correlation functions and given in Table V. It can be observed that the value of the perpendicular component, τ_ω, changes by a factor of 0.7 when the concentration of quinuclidine is increased, whereas the change for the parallel component is 0.4. The implications of these changes will be further discussed in the section on the molecular reorientations. It can be observed, in Figure 9, that the motion of quinuclidine in both systems is clearly anisotropic. This behavior has been previously observed in molecules with very different components of the moment of inertia tensor. One such example is acetonitrile ($I_\parallel/I_\perp = 10$) where the ratio between the components, $\tau_{\omega_\parallel}/\tau_{\omega_\perp}$ was found to be close to 2.0.[45] However, in quinuclidine the ratio between the moments of inertia is 1.06, and the large anisotropy in the angular velocity (1.9 and 2.9 for the high and the low concentration, respectively) originates in strong interactions with the solvent. Furthermore, the corresponding anisotropy in the benzene simulation was found to be 1.2. The cage effect observed in the angular velocity correlation functions originates in strong intermolecular torques. This effect is expected for the perpendicular component, since the reorientation of the symmetry axis involves breaking or stretching of the hydrogen bonds, formed between quinuclidine and water. The parallel component of the angular velocity is much less hindered, which is also clearly apparent in the time correlation function.

The angular velocity correlation functions for water (not shown) in the mixtures and in pure water are practically identical. This is surprising, considering the differences both in translational

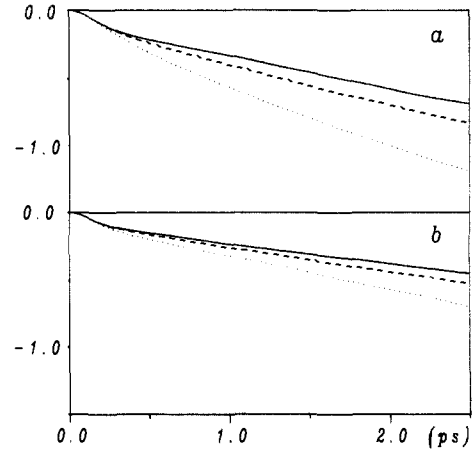

Figure 10. The reorientation correlation functions plotted as $\ln[C_m(t)]$ for quinuclidine: (a) 2 mol % and (b) 6 mol %, (—) $m = 0$, (--) $m = 1$, (···) $m = 2$.

motion and in viscosity and can probably be explained by the generally poor description of dynamic properties by the SPC water model.

4.5. Reorientational Motion. The reorientational motion of the molecules is described by using the normalized time correlation functions, $C_{lm}(t)$, defined by

$$C_{lm}(t) = \langle \hat{Y}_{lm}[\Theta(t)\varphi(t)]\,\hat{Y}^*_{lm}[\Theta(0)\varphi(0)]\rangle = \langle \sum_{m'} D^{*2}_{mm'}[\Omega_{LM}(t)]\,D^2_{mm'}[\Omega_{LM}(0)]\rangle \quad (6)$$

where $\hat{Y}_{lm}(\Theta,\varphi)$ are the spherical harmonics with the axes fixed in the molecule and z component along the symmetry axis, $D_{mm'}(\Omega)$ are the Wigner rotation matrices, and $\Omega_{LM}(t)$ are the Euler angles for the transformation from the laboratory to the molecular coordinate system. The Wigner rotation matrices have been calculated from the Cayley–Klein parameters which are related to the quaternions.[46]

The time correlation functions with the different l values correspond to the properties measured by various spectroscopic methods. For the nuclear spin relaxation the appropriate functions are those with $l = 2$ and the different m values ($m = 0, 1, 2$). The reorientational motion of symmetric top molecules, in the small step diffusion limit,[47] can be separated into the reorientation of the symmetry axis denoted as molecular tumbling and into the reorienation about the symmetry axis, denoted as spinning motion.

The tumbling motion is described by $C_{20}(t)$ alone, whereas combination of all three correlation functions is necessary for the evaluation of the spinning motion. In Figure 10 the reorientational correlation functions for $l = 2$ and $m = 0, 1, 2$ are plotted on a logarithmic scale. For a diffusive reorientation the correlation functions are exponential, and the plots should be linear. This is indeed the case at long times ($t > 2.5$ ps), whereas the short time behavior is mainly inertial. From the plots it can clearly be seen that the molecular reorientations of quinuclidine in water are anisotropic. (Isotropic motion gives identical plots for different m values.)

In our previous simulation of quinuclidine in benzene, we found an essentially isotropic motion of the molecule. This is not surprising since quinuclidine is not expected to be involved in any strong intermolecular interactions with benzene. The hydrogen bonds formed in water and other similar solvents, such as methanol and chloroform,[12] restrict the tumbling motion strongly, whereas the spinning motion is much less affected. The large reorientational anisotropy is also expected considering the anisotropy in the angular velocity correlation functions. A quantitative measure of the anisotropy can be obtained from the reorientational correlation times, calculated from the integral of the corresponding

(45) Böhm, H. J.; Lynden-Bell, R. M.; Madden, P. A.; McDonald, I. R. *Mol. Phys.* **1984**, *51*, 761–777.

(46) Goldstein, H. *Classical Mechanics*, 2nd ed.; Addison-Wesley: Reading, MA, 1981; Chapter 4.

(47) Woessner, D. E. *J. Chem. Phys.* **1962**, *37*, 647–654.

Table VI. Experimental ^{14}N Correlation Times and the Viscosities of the Solutions at 25 °C

concn (mol %)	τ (ps)	η (cP)	τ/η
0.2	11.4	0.930	1.00
1.0	13.2	1.137	0.94
2.0	17.1	1.411	0.99
3.0	21.4	1.759	0.99
6.0	28.2	3.039	0.75
10.0	34.8	5.244	0.54

functions. These correlation times can be compared with experimental values obtained from nuclear spin measurements. The correlation time for the reorientation of a vector fixed in a symmetric top molecule and measured in an NMR experiment is given by

$$\tau_c = \frac{1}{4}[\cos^2\theta - 1]^2\tau_{20} + 3\cos^2\theta\sin^2\theta\tau_{21} + \frac{3}{4}\sin^4\theta\tau_{22} \quad (7)$$

where θ is the angle between the vector and the symmetry axis, and correlation times τ_{20}, τ_{21}, and τ_{22} are calculated from the corresponding correlation functions and are included in Table V.

We have performed a number of measurements of ^{14}N relaxation rates, at different concentrations of quinuclidine. These measurements provide a correlation time that is characteristic to the reorientation of the symmetry axis or the molecular tumbling and can therefore be directly compared with τ_{20}, computed from the correlation function of the simulation. In Table VI the experimental values for the tumbling correlation times are given together with the measured viscosities for different concentrations of quinuclidine. The correlation times *increase* significantly with the concentration, and a large increase of the viscosity is also observed. However, the effect of the increased viscosity can be removed by division by the viscosity (and normalization with respect to the lowest concentration value). This ratio, which is also included in Table VI, is fairly constant for the four lowest concentrations and *decreases* significantly for the two highest concentrations. A possible explanation is the effect of an increased motional freedom in the hydrocarbon-rich part of the solution. In dilute solution, all quinuclidine molecules are effectively in contact with water, which hinders the reorientations by the formation of hydrogen bonds.

The correlation time for the reorientation of the symmetry axis, τ_{20}, obtained from the simulations are 4.3 and 7.3 ps in 2 and 6 mol % solutions, respectively. The differences between the simulated and measured values seem to be very large. These differences reduce somewhat since the experiments are performed at 25 °C, whereas the average temperatures in the simulations are 45 and 36 °C for the low and the high concentration, respectively. The poor agreement in the description of the dynamical properties, when using SPC water as solvent was previously reported in MD simulations of a small calcium complex[48] and parvalbumin[49] in aqueous solutions. However, the concentration dependence of the tumbling correlation times of quinuclidine seems to be in good agreement with the experiments. The ratio between the experimental and the temperature-scaled simulated values of τ_{20} is 3.7 for both concentrations.

The spinning and tumbling motions of quinuclidine can be evaluated, assuming the diffusion limit, from the correlation times using the relation

$$\tau_{2m}^{-1} = 6R_\perp + m^2(R_\parallel - R_\perp) \quad (8)$$

where $R_\perp$ is the perpendicular component of rotational tensor and $R_\perp$ is the parallel component. Since τ_{20} provides $R_\perp$ directly, the combination of τ_{20} and τ_{21} or τ_{22} gives $R_\parallel$. By using the values in Table V and eq 8 the values of $R_\parallel$ can be evaluated. In more dilute solution $R_\perp = 3.9 \times 10^{10}$ s^{-1}, whereas $R_\parallel = 9.7 \times 10^{10}$ and 8.0×10^{10} s^{-1} obtained from τ_{21} and τ_{22}, giving an anisotropy ratio defined as $R_\parallel/R_\perp$ of 2.5 and 2.0, respectively. These values are too small compared with the experiments performed on quinuclidine in methanol or chloroform,[13] where the corresponding ratio was 10. In the more concentrated solution $R_\perp = 2.3 \times 10^{10}$ s^{-1} and $R_\parallel = 5.7 \times 10^{10}$ s^{-1} and 5.1×10^{10} s^{-1} from τ_{21} and τ_{22} giving $R_\parallel/R_\perp$ 2.5 and 2.2, respectively. The consistence of $R_\parallel$ obtained from τ_{21} and τ_{22} indicates that the reorientations indeed proceed in the small-step diffusion limit.

A more detailed discussion of theoretical and experimental aspects of the reorientational motion of quinuclidine in polar and nonpolar solvents is given in ref 50. The reorientations of water in the mixture are almost identical with these of pure water, and the discussion of the dynamics of water in a simulation with the SPC interaction model have been previously reported.[39]

5. Conclusions

Molecular dynamics simulations of 1.2 and 3.5 M aqueous solutions of quinuclidine are reported. An increased ordering of water structure has been observed. The effect of increased structuring of water and decreased entropy, called hydrophobic effect, is well-known in aqueous solutions of hydrocarbons. This effect increases significantly with the increased concentration. Hydrogen bond formation between quinuclidine and water is observed as well as a tendency of quinuclidine molecules to aggregation in the high concentration solution. The aggregation of quinuclidine is most likely due to the minimized contact of water with the hydrocarbon part. Large concentration effects in absorption and fluorescence spectra and the kinetic behavior of the fluorescence signal suggest rearrangement of quinuclidine molecules in water at high concentrations into weakly bound clusters. The translational motion of water in the mixtures is retarded compared with the pure liquid. This effect has been observed previously in similar solutions, both by computer simulations and by experimental methods.

Reorientation of quinuclidine in aqueous solutions is clearly anisotropic, due to hydrogen bonds formed with water. The erroneously high absolute values of the dynamic parameters are due to the viscosity of the SPC water, which is approximately a factor of three below the experimental values. Their concentration dependence, however, is correct. The model for quinuclidine–water interactions is based on quantum chemical calculations performed on ammonia/water system; however ammonia is a weaker proton acceptor compared to trimethylamine and quinuclidine. Therefore, the hydrogen bonds formed in the simulated system are probably too weak. Furthermore, we have not made any attempt to optimize the interactions between the hydrocarbon part and water. The improvement of this simulation as well as simulations of other water solutions is severely limited by existing models for water.

Acknowledgment. This work has been supported by the Swedish Natural Science Research Council. We are indebted to Profs. Peter Stilbs for providing us with the diffusion coefficients and Jozef Kowalewski for his encouragment and valuable discussions.

Registry No. H_2O, 7732-18-5; quinuclidine, 100-76-5.

(48) Marchese, F. T.; Mehrotra, P. K.; Beveridge, D. L. *J. Phys. Chem.* **1984**, *88*, 5692-5702.
(49) Ahlström, P.; Teleman, O.; Jönsson, B.; Forsén, S. *J. Am. Chem. Soc.* **1987**, *109*, 1541-1551.
(50) Maliniak, A. Doctoral Thesis, 1988, University of Stockholm.